Minimal 3D Dubins Path with Bounded Curvature and Pitch Angle

Petr Váňa,[1]   Armando Alves Neto,[2]   Jan Faigl,[1]   Douglas G. Macharet[3]

Abstract— In this paper, we address the problem of finding cost-efficient three-dimensional paths that satisfy the *maximum allowed curvature* and the *pitch angle* of the vehicle. For any given initial and final configurations, the problem is decoupled into finding the horizontal and vertical parts of the path separately. Although the individual paths are modeled as two-dimensional Dubins curves using closed-form solutions, the final 3D path is constructed using the proposed local optimization to find a cost-efficient solution. Moreover, based on the decoupled approach, we provide a lower bound estimation of the optimal path that enables us to determine the quality of the found heuristic solution. The proposed solution has been evaluated using existing benchmark instances and compared with state-of-the-art approaches. Based on the reported results and lower bounds, the proposed approach provides paths close to the optimal solution while the computational requirements are in hundreds of microseconds. Besides, the proposed method provides paths with fewer turns than others, which make them easier to be followed by the vehicle's controller.

I. Introduction

The interest and research in Unmanned Aerial Vehicles (UAVs) is increasingly growing, mainly due to the decrease in the cost, weight, size, and improvement in the performance of actuators, sensors, and computational resources. Also, considering their full range of applications, these vehicles address a niche of employment that cannot be fulfilled by any other mobile robots. In this context, three-dimensional path planning is a fundamental task for robots moving in the three-dimensional space, like fixed-wing UAVs but also underwater gliders [1]. Even though it might be possible for such robots to navigate in the environment reactively, the competence of planning efficient paths is an essential feature for applications such as monitoring and surveillance [2], [3], [4]. In addition to the requirement that the path must be cost-efficient (e.g., the shortest or fastest one), the essential goal is that the path must be *feasible* by the particular vehicle. Therefore, it is crucial to determine a path with a minimal length while still satisfying the vehicle's motion constraints.

[1]Petr Váňa and Jan Faigl are with the Faculty of Electrical Engineering, Czech Technical University, 166 27 Prague, Czech Republic. E-mails: {vanapet1,faiglj}@fel.cvut.cz

[2]A. Alves Neto is with the Department of Electronic Engineering, Universidade Federal de Minas Gerais, MG, Brazil. E-mail: aaneto@cpdee.ufmg.br

[3]D. G. Macharet is with the Computer Vision and Robotics Laboratory (VeRLab), Department of Computer Science, Universidade Federal de Minas Gerais, MG, Brazil. E-mail: doug@dcc.ufmg.br
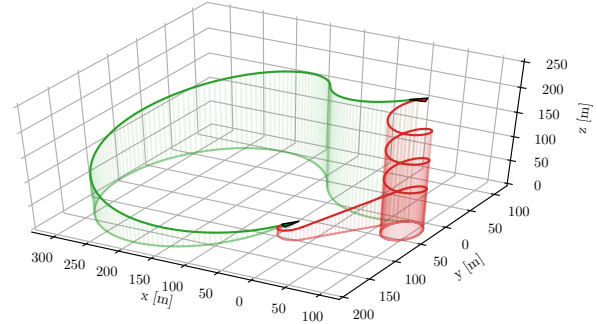
Fig. 1. Example paths connecting initial and final (goal) configurations by the Dubins airplane model [5] (red) and the proposed approach (green) for the problem instance Short 3 defined in Table I.

For fixed-wing vehicles operating in two-dimensional space, the motion curvature can be limited by a particular minimum turning radius, and the Dubins vehicle model [6] can be utilized to determine the optimal maneuver connecting two locations with the prescribed leaving and arrival angles of the vehicle. In the case of the generalization of Dubins maneuver into three-dimensional space, the climb (or dive) angle is the fundamental constraint that refers to the rate of the altitude change, and that is severely restricted for some particular aerial and underwater vehicles.

In this paper, we address the problem of finding a 3D curvature-constrained path satisfying both (i) the maximum allowed curvature and (ii) minimum and maximum pitch angle (hereafter referred to as climb angle). The proposed methodology is based on the decomposition of the problem into a separate calculation of 2D paths on horizontal and vertical planes using optimal Dubins maneuvers [6] with two separate turning radii. These paths are later combined into one final feasible 3D path using relatively straightforward, yet efficient, iterative optimization technique. Moreover, lower and upper bound estimations of the optimal 3D maneuver are proposed utilizing the same decoupled approach. Based on the empirical evaluation of the proposed and state-of-the-art approaches [5], [7], including numerically found solutions [8], the newly proposed method provides competitive solutions. Besides, the paths found by the proposed method contain fewer turns in comparison to existing heuristics, see Fig. 1, which may help a conventional flight controller to follow the path.

The rest of the paper is structured as follows. The next section overviews the related work. The used notation, together with the problem statement, is presented in Section III. The proposed optimization procedure with lower and upper bound estimations are described in Section IV. Results on the numerical analysis are reported in Section V, and concluding remarks in Section VI.

II. Related Work

The addressed problem is related to the motion planning for autonomous vehicles that is a subject of many investigations with several approaches proposed in the literature [9]. A considerable number of works addressing the generation of feasible paths for non-holonomic vehicles are based on heuristic approaches [10] including randomized sampling-based [11], [12] and evolutionary [13], [14] methods. Although heuristic methods might provide feasible paths quickly, it is at the cost of neglecting the path length.

A systematic study of the shortest path for a vehicle with the limited turning radius has been presented by L. E. Dubins in 1957 [6]. He proved the optimal curve between two adjacent points in $\mathbb{R}^2$ with the prescribed leaving and arrival orientation of the vehicle (also called Dubins maneuver) could be composed only of a straight line segment (S) and arcs (C) with the minimum turning radius, and two basic types of the maneuvers exist CSC and CCC.

The original Dubins vehicle model [6] (limited to 2D space) has been extended into the three-dimensional case called the *Dubins airplane model* where, in addition to the curvature limitation, the climb-rate constraint is also considered [15]. The Dubins airplane model allows the climb-rate to be changed abruptly, and thus the resulting trajectories are not necessarily smooth. Contrarily to the 2D, there is not a proven closed-form solution in the literature to obtain the minimum path connecting any two arbitrary configurations in the 3D space, respecting both curvature and pitch angle constraints. Therefore, several approaches have been proposed to tackle this challenging problem.

An approach based on the minimum 2D path between two configurations in $\mathbb{R}^2$ (the projection of the original poses) is proposed in [16]. The calculated path is then extended to 3D by incrementing the altitude (z value) linearly along the previously computed 2D path. However, such a path might not respect the pitch angle constraint, especially for configurations that are spatially close in the horizontal plane.

A sub-optimal approach to generate paths between two 3D poses dealing with both curvature and pitch constraints is proposed in [17]. The final path is considered as a union of three possible subpaths: two subpaths at the extreme points to address the pitch angle constraint and one in the middle of the final path to deal with the horizontal displacement.

The optimal path planning in the 3D is addressed by the authors of [8] that propose geometrical and numerical approaches to generate 3D paths. The geometrical approach only fulfills the curvature constraint [18], while the numerical approach also incorporates the pitch angle constraint. The authors claim that their numerical approach provides optimal solutions for large enough number of samples; however, no formal proof ensuring the convergence is provided.

In [5], 3D Dubins paths are calculated by adding a helical path at the beginning or end of the path to respect the pitch angle constraint. However, initial and final pitch angles are not taken into account. Similarly, the authors of [7] present the Real-time Dynamic Dubins-Helix (RDDH), a 3D Dubins approximation also based on the helical paths. Like in [17], the resulting path is composed of three subpaths: two semicircles and a Dubins-Helix added into the final curve.

In the presented work, we follow the idea of utilizing 2D Dubins maneuver; however, contrary to the previous approaches, the method decouples planning the 3D path according to its displacement on both horizontal and vertical planes. The method utilizes local optimization of the horizontal turning radius to prolong the path such that the maximum curvature and pitch angle constraints are fulfilled, if necessary. Moreover, based on the proposed decoupled approach, we propose both lower and upper bound estimations of the optimal 3D Dubins maneuver that enable us to evaluate the quality of the heuristically found solutions. Regarding the results presented in Section V, the proposed method provides competitive solutions, or even better, while the final paths contain fewer turns than, e.g., solutions provided by [5].

III. Used Notation and Problem Statement

The problem of finding the 3D optimal path for curvature-constrained vehicles must consider not only the vehicle's position in space but also its departure (arrival) orientation from the initial (final) location. The notion of the special Euclidean group $\mathrm{SE}(n)$ is therefore utilized to represent the homeomorphic topological space where the path planning is performed. Both the minimum turning radius and pitch angle are addressed, and therefore, the configuration of the vehicle is denoted as $\mathbf{q}_k \in \langle x_k, y_k, z_k, \psi_k, \gamma_k \rangle$ to represent the pose k in $\mathrm{SE}(3)$, where $\langle x_k, y_k, z_k \rangle$ are spatial coordinates of the vehicle, ψ_k is the vehicle's heading and γ_k is the vehicle's pitch. Since we consider generations of 2D paths, the projection of the configuration $\mathbf{q}_k \in \mathrm{SE}(3)$ into $\mathrm{SE}(2)$ corresponding with the horizontal XY plane is a function $\mathcal{P}(\mathbf{q}_k) = \langle x_k, y_k, \psi_k \rangle$ that maps $\mathbf{q}_k$ into $\mathcal{P}(\mathbf{q}_k) \in \mathrm{SE}(2)$. We further denote the Euclidean magnitude of a vector as $|\cdot|$, 2D Dubins function proposed in [6] as $\mathcal{D}(\cdot)$ and $\{k\}_{2\pi}$ for the modulus after the division of an angle k by 2π.

The addressed path planning problem is considered for a given obstacle-free environment, where the motion constraints impose the only restrictions for the vehicle. The problem is to determine a minimal *smooth* regarding the variation of ψ_k and γ_k path from the initial pose $\mathbf{q}_i$ to the final pose $\mathbf{q}_f$ such that the curvature of the path in the horizontal plane is limited by the minimum turning radius $\rho_{\min}$, and the pitch angle is constrained in the interval $\Gamma = [\gamma_{\min}, \gamma_{\max}]$.

The requested path is a parametric curve $\vec{r}(t) : [0, 1] \to \mathbb{R}^3$ from the class $\mathbb{C}^1$ (the first derivatives of the curve are continuous) and the ends of the path are constrained by the initial $\vec{r}(0) = \mathbf{q}_i$ and final $\vec{r}(1) = \mathbf{q}_f$ configurations.

Regarding the physics of the vehicle, the curvature $\kappa(t)$: $\mathbb{R}^n \to \mathbb{R}_0^+$ can be defined as the quantity directly proportional to the lateral acceleration of the robot in the space. The maximum curvature is thus inversely proportional to the minimum turning radius $\rho_{\min}$ of the curve, and the curvature function in the horizontal plane can be expressed as

$$\kappa(t) = \frac{|\dot{r}(t) \times \ddot{r}(t)|}{|\dot{r}(t)|^3}. \tag{1}$$

The vehicle *pitch* denotes the climb (or dive) angle of the vehicle, and it is proportional to the ascent (or descent) rate of the vehicle in $\mathbb{R}^3$. Therefore, it is the fundamental constraint for a vehicle with the bounded angle of the attack, such as fixed-wing aircraft. The pitch angle is constrained by the given interval $\Gamma = [\gamma_{\min}, \gamma_{\max}]$ where particular values of $\gamma_{\min}$ and $\gamma_{\max}$ depend on many factors such as velocity or spatial orientation of the vehicle. The feasibility conditions on the requested path $\vec{r}(t)$ to respect all the considered motion constraints of the vehicle can be expressed as

$$\kappa(t) \leq \rho_{\min}^{-1} \quad \text{and} \quad \gamma(t) \in \Gamma. \tag{2}$$

IV. PROPOSED SOLUTION TO THE 3D PATH PLANNING

The proposed approach to finding a feasible Dubins path in the three-dimensional space is based on the separation of the path into its horizontal and vertical parts. The overall idea is similar to [5], where the horizontal projection of the final path is computed as the 2D Dubins path, and the vertical profile is an interpolation between the altitude at the initial and final location. However, the interpolation might provide unfeasible paths because abrupt changes in the pitch angle in [5]. The herein proposed heuristic addresses this issue by computing the vertical profile, also like the 2D Dubins path, to ensure a smooth connection at the endpoints. Thus, it respects both initial and final configurations of the vehicle, which can be further utilized in multi-goal planning. Furthermore, the horizontal radius ρ_h and vertical turning radius ρ_v are addressed separately such that the final length is minimized while the maximally allowed curvature is not exceeded.

The proposed method consists of two fundamental steps. Initially, the horizontal curve $\mathcal{D}_h$ of the 3D curve is computed as the 2D Dubins path connecting the projections of $\mathbf{q}_i$ and $\mathbf{q}_f$ into the XY (*latero-directional*) plane using the horizontal turning radius ρ_h. Secondly, the altitude profile of the 3D curve is also computed as the 2D Dubins path with the minimum vertical turning radius ρ_v. In the vertical case, the configurations are projected into the SZ (*longitudinal*) plane, where the axis S represents the traveled horizontal distance, and the axis Z represents the altitude, i.e., the longitudinal plane captures the changes in the altitude along the traveled path in the latero-directional plane, see Fig. 2.

The separation of the original 3D path planning problem to its horizontal and vertical parts helps to find an effective heuristic algorithm because of the closed-form expression of the 2D Dubins curves [6] can found the solution in less than microsecond as reported in [19]. Formally, the 2D Dubins curve is the shortest curve $\mathcal{D} : [0,1] \to \mathrm{SE}(2)$ from the initial configuration $\mathcal{D}(0)$ to the final configuration $\mathcal{D}(1)$.

The Dubins path is a continuously differentiable function, and thus the curve is from the class $\mathbb{C}^1$. Let the length of the curve be $\mathcal{L}(\mathcal{D})$ for the rest of the paper, and it can be defined as

$$\mathcal{L}(\mathcal{D}) = \int_1^0 \left| \dot{\mathcal{D}}^{XY}(t) \right| \delta t, \tag{3}$$
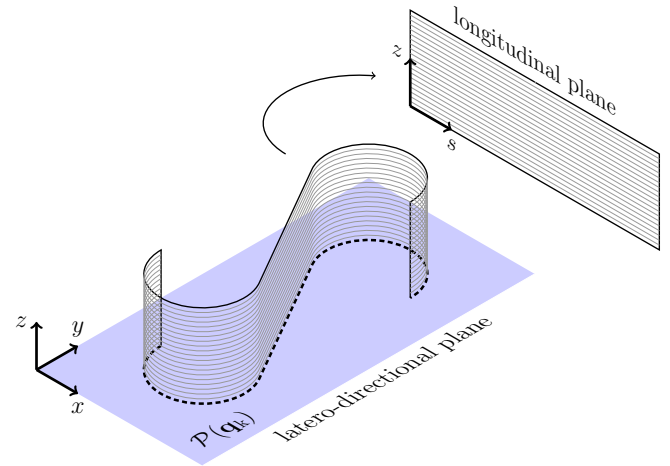

Fig. 2. Projection of the 3D curve into the latero-directional (horizontal) and longitudinal (vertical) planes.

where $\dot{\mathcal{D}}^{XY}(t)$ stands for the derivative of the position in the XY plane defined by the Dubins path $\mathcal{D}$.

Although the original problem is decoupled into two sub-problems, they are not entirely independent because of the maximal curvature constraint (2). The curvature depends on the radii ρ_h and ρ_v, and also pitch angle γ because for $\gamma \neq 0$, the horizontal and vertical turns are not perpendicular. The particular curvature κ can be computed as

$$\kappa = \sqrt{\cos^4(\gamma)\, \rho_h^{-2} + \rho_v^{-2}}. \tag{4}$$

The worst case occurs for $\gamma = 0$; then, the following constrains limits the turning radii independently on γ angle

$$\rho_{\min}^{-2} \geq \rho_h^{-2} + \rho_v^{-2}. \tag{5}$$

The procedure to find the decoupled solutions as Dubins curves $\mathcal{D}_h$ and $\mathcal{D}_v$ is depicted in Algorithm 1 in which the method Dubins2D returns the shortest Dubins path for the requested initial and final configurations in SE(2) and the specified minimum turning radius [20].

Algorithm 1: Decoupled($\mathbf{q}_i, \mathbf{q}_f, \rho_{\min}, \rho_h$)

Output: $\mathcal{D}_h$ – Horizontal Dubins maneuver
Output: $\mathcal{D}_v$ – Vertical Dubins maneuver

// Compute both maneuvers separately
1   $\mathcal{D}_h \leftarrow \text{Dubins2D}\left(\langle x_i, y_i, \psi_i \rangle, \langle x_f, y_f, \psi_f \rangle, \rho_h\right)$
2   $\rho_v \leftarrow \left(\rho_{\min}^{-2} - \rho_h^{-2}\right)^{-\frac{1}{2}}$
3   $\mathcal{D}_v \leftarrow \text{Dubins2D}\left(\langle 0, z_i, \gamma_i \rangle, \langle \mathcal{L}(\mathcal{D}_h), z_f, \gamma_f \rangle, \rho_v\right)$
4   **return** $\mathcal{D}_h, \mathcal{D}_v$

The curves determined by the decoupled approach guarantee the maximal curvature is not exceeded. However, the vertical profile given by $\mathcal{D}_v$ may violate the pitch angle constraint (given by Γ) if the straight part of the CSC type is too steep or if the CCC type occurs. If the length of the horizontal maneuver $\mathcal{L}(\mathcal{D}_h)$ is not sufficient to adjust the altitude with the pitch angle in the range of Γ and meet initial and final pitch angles γ_i, γ_f, the horizontal radius ρ_h is increased to prolong the vertical part. The proposed heuristic

for finding the 3D Dubins path consists of the following three parts that are summarized in Algorithm 2.

1) An initial feasible solution is found such that the horizontal turning radius ρ_h is incrementally increased until the length of the horizontal curve $\mathcal{D}_h$ is sufficient to find its vertical counterpart that is feasible. The Decoupled procedure listed in Algorithm 1 is utilized and the feasibility of vertical curve $\mathcal{D}_v$ is checked by the procedure IsFeasible($\mathcal{D}_v, \Gamma$) to meet (2).

2) The length of the found path is improved by a local optimization using the hill-climbing technique such that the most beneficial horizontal radius ρ_h is selected. The optimization is stopped when the step Δ is less than a minimum change of the radius Δ_{min}.

3) The final 3D path is constructed as a combination of horizontal and vertical Dubins curves $\mathcal{D}_h$ and $\mathcal{D}_v$, respectively.

Algorithm 2: Dubins3D($\mathbf{q}_i, \mathbf{q}_f, \rho_{\min}, \Gamma$)

Input: $\mathbf{q}_i$, $\mathbf{q}_f$ – Initial and final configurations
Input: $\rho_{\min}$, Γ – Curvature constraint: the minimum turning radius and allowed pitch angle
Output: $\vec{r}(t)$ – Final 3D Dubins path

1   $\rho_h \leftarrow \rho_{\min}$ `// Init. horizontal radius` ρ_v
    `// 1) Increase` ρ_h `to get a feasible sol.`
2   **repeat**
3     $\rho_h \leftarrow 2\,\rho_h$
4     $\mathcal{D}_h, \mathcal{D}_v \leftarrow$ Decoupled($\mathbf{q}_i, \mathbf{q}_f, \rho_{\min}, \rho_h$)
5   **until** IsFeasible($\mathcal{D}_v, \Gamma$);
    `// 2) Local optim. of the horiz. radius`
6   $\Delta = 0.1\,\rho_{\min}$ `// Init. the update step`
7   **while** $|\Delta| > \Delta_{min}$ **do**
8     $\rho'_h \leftarrow \max(\rho_{\min}, \rho_h + \Delta)$
9     $\mathcal{D}'_h, \mathcal{D}'_v \leftarrow$ Decoupled($\mathbf{q}_i, \mathbf{q}_f, \rho_{\min}, \rho'_h$)
10   **if** IsFeasible($\mathcal{D}'_v, \Gamma$) and $\mathcal{L}(\mathcal{D}'_v) < \mathcal{L}(\mathcal{D}_v)$ **then**
11      $\rho_h \leftarrow \rho'_h$
12      $\mathcal{D}_h, \mathcal{D}_v \leftarrow \mathcal{D}'_h, \mathcal{D}'_v$
13      $\Delta \leftarrow 2\,\Delta$
14   **else**
15      $\Delta \leftarrow -0.1\,\Delta$
    `// 3) Construct the final path`
16   $s_h \leftarrow \mathcal{L}(\mathcal{D}_h)$
17   $\vec{r}(t) : t \rightarrow \left\langle \mathcal{D}_h^{XY}(\mathcal{D}_v^S(t)/s_h), \mathcal{D}_v^Z(t) \right\rangle$
18   **return** $\vec{r}(t)$

A. Proposed Lower Bound

In addition to the heuristic solution of the 3D Dubins path, the proposed decoupled approach can also be utilized for estimating the lower bound of the optimal path length. The idea is based on setting both horizontal and vertical turning radii to their minimal values in Algorithm 1. For the vertical radius, its minimum value is given by the minimum turning radius $\rho_{\min}$. On the other hand, the horizontal radius can be even smaller for $\gamma \neq 0$, when the turn is a spiral and the minimum value $\widehat{\rho_h}$ can be derived from (4) according to the

maximum absolute value of the pitch angle as

$$\widehat{\rho_h} = \cos^2(\max(|\gamma_{\min}|, |\gamma_{\max}|))\,\rho_{\min}. \tag{6}$$

Once the minimum turning radii are set, both 2D Dubins paths can be constructed separately, and the maximum path length can be selected as the lower bound. However, we can further tighten the lower bound value for the 2D Dubins path in the vertical plane by a prolongation of the curve to meet the pitch angle constraint. Therefore, we introduce the procedure Vertical that provides the shortest possible prolongation (or none if not necessary) along the S-axis for the final configuration given by $\mathcal{L}(\mathcal{D}_h)$ to create a space for the altitude change within the pitch angle interval Γ. Such a prolongation can be found by a closed-form expression, and thus the proposed lower bound can be computed quickly. The method is summarized in Algorithm 3.

Algorithm 3: LowerBound($\mathbf{q}_i, \mathbf{q}_f, \rho_{\min}, \Gamma$)

Output: LB – Lower bound length

1   $\widehat{\rho_h} \leftarrow \cos^2(\max(|\gamma_{\min}|, |\gamma_{\max}|))\rho_{\min}$ `// Use (6)`
2   $\mathcal{D}_h \leftarrow$ Dubins2D ($\langle x_i, y_i, \psi_i \rangle, \langle x_f, y_f, \psi_f \rangle, \widehat{\rho_h}$)
3   $\mathcal{D}_v \leftarrow$ Vertical ($\langle 0, z_i, \gamma_i \rangle, \langle \mathcal{L}(\mathcal{D}_h), z_f, \gamma_f \rangle, \rho_{\min}, \Gamma$)
4   **return** $\max(\mathcal{L}(\mathcal{D}_h), \mathcal{L}(\mathcal{D}_v))$

B. Proposed Upper Bound

The decoupled approach also enables to compute an upper bound value on the 3D Dubins path length. The heuristic Algorithm 2 is based on a local optimization that iteratively computes the decoupled solution; hence, an upper bound computed from a single decoupled solution can be significantly less computationally demanding.

Algorithm 4: UpperBound($\mathbf{q}_i, \mathbf{q}_f, \rho_{\min}, \Gamma$)

Output: UB – Upper bound length

1   **if** $|\langle x_i, y_i \rangle - \langle x_f, y_f \rangle| < 4\sqrt{2}\,\rho_{min}$ **then**
2   **return** ∞
3   $\mathcal{D}_h \leftarrow$ Dubins2D ($\langle x_i, y_i, \psi_i \rangle, \langle x_f, y_f, \psi_f \rangle, \sqrt{2}\,\rho_{\min}$)
4   $\mathcal{D}_v \leftarrow$ Vertical ($\langle 0, z_i, \gamma_i \rangle, \langle \mathcal{L}(\mathcal{D}_h), z_f, \gamma_f \rangle, \sqrt{2}\,\rho_{\min}, \Gamma$)
5   **return** $\max(\mathcal{L}(\mathcal{D}_h), \mathcal{L}(\mathcal{D}_v))$

Particular values of both turning radii need to be selected to guarantee the curvature constraint is always met. It can be achieved by setting both radii to the same value which results in the maximal curvature for $\gamma = 0$, i.e., $\rho_h = \rho_v = \sqrt{2}\,\rho_{\min}$, see (4). Then, the horizontal and vertical 2D Dubins curves can be computed in the same manner as for the lower bound. However, the horizontal distance between the initial and final configurations need to be at least $4\,\rho_h$ to guarantee that the horizontal curve is of the CSC type, which ensures a feasible solution is always constructible. Otherwise, the horizontal curve may not be possible to prolong precisely by a given value because the length of the Dubins curve is a piecewise-continuous function, and discontinuities occur on the boundary between CSC and CCC types. Thus, the upper bound computation is limited to the cases of significantly apart configurations. The proposed upper bound method is summarized in Algorithm 4.

V. Numerical Analysis

The proposed method for solving the addressed 3D Dubins path planning problem has been numerically evaluated using the existing benchmark instances presented in [7], also listed in Table I to make the paper self-contained and results easier to replicate. Instances are divided into two groups denoted *Long* and *Short* depending on the spatial distance of the initial configuration q_i and the final configuration q_f projected into the horizontal plane. For instances from the *Long* group, the distance between q_i and q_f is much longer than the corresponding difference in z_i and z_f.

TABLE I
Benchmark Instances for 3D Dubins Path Planning Problem

Name	$q_i = \langle x_i, y_i, z_i, \psi_i, \gamma_i \rangle$	$q_f = \langle x_f, y_f, z_f, \psi_f, \gamma_f \rangle$
Long 1	$(200, 500, 200, 180°, -5°)$	$(500, 350, 100, 0°, -5°)$
Long 2	$(100, -400, 100, 30°, 0°)$	$(500, -700, 0, 150°, 0°)$
Long 3	$(-200, 200, 250, 240°, 15°)$	$(500, 800, 0, 45°, 15°)$
Long 4	$(-300, 1200, 350, 160°, 0°)$	$(1000, 200, 0, 30°, 0°)$
Long 5	$(-500, -300, 600, 150°, 10°)$	$(1200, 900, 100, 300°, 10°)$
Short 1	$(120, -30, 250, 100°, -10°)$	$(220, 150, 100, 300°, -10°)$
Short 2	$(380, 230, 200, 30°, 0°)$	$(280, 150, 100, 200°, 0°)$
Short 3	$(-80, 10, 250, 20°, 0°)$	$(50, 70, 0, 240°, 0°)$
Short 4	$(400, -250, 600, 350°, 0°)$	$(600, -150, 300, 150°, 0°)$
Short 5	$(-200, -200, 450, 340°, 0°)$	$(-300, -80, 100, 100°, 0°)$

The same values for the minimum turning radius $\rho_{min} = 40\,\mathrm{m}$ (defining the maximal path curvature) and pitch angle interval $\Gamma = [-15°, 20°]$ as in [7] are used in the herein presented evaluation results. In addition to the proposed method, the existing approaches Real-time Dynamic Dubins-Helix (RDDH) [7] and the numerical method proposed in [8] (denoted Numerical) have been selected for comparison.

Two lower bounds and one upper bound are also included in the comparison. The first lower bound is denoted $\mathrm{LB_{Num}}$, and it is computed as the shortest 3D curvature-constrained path [18] but without considering the limitation on the pitch angle. The second lower bound (denoted LB) is determined by the method proposed in Section IV-A, and it is computed as the longer value of the path length from the separately computed minimal horizontal and vertical paths. Finally, the upper bound UB, introduced in Section IV-B, allows us to quickly estimate the path length for instances with configurations more than $4\rho_{min}$ apart in the horizontal plane.

The evaluation results are listed in Table II, where the %GAP column indicates the relative gap in the percentage points of the proposed solution to the tighter lower bound value provided either by the $\mathrm{LB_{Num}}$ or by the proposed LB. In addition, we further distinguish the relative gap computed only from the proposed lower bound LB and upper bound UB as $\mathrm{GAP_b}$ to provide an overview of how quickly the solution quality can be estimated using the proposed decoupled approach. The tighter lower bound values are highlighted in bold similarly as the lowest path length. The computational requirements T_{LB}, T_{UB}, and T are reporeted for the implementation[1] in Julia 1.2 executed on the Intel i5-7600K CPU running at up to $4.2\,\mathrm{GHz}$.

[1] Source codes in Julia language are available at [21], and together with related software at https://purl.org/comrob/sw.

The results support the efficiency of the proposed decoupled approach further accompanied by iterative optimization of the turning radius. The proposed method outperforms the other methods for most of the test instances. The proposed lower bound is tighter for the Short instances than the lower bound based on [18], which can be considered as more challenging because, in these instances, additional helical parts might be needed to reach the final configurations at relatively high altitude from the initial configurations. The proposed upper bound provides interesting insights that the RDDH [7] provides worse results for some cases that indicate it should be accompanied by the proposed upper bound, which is computationally efficient.

An example of the determined 3D Dubins path for the benchmark instance Long 3 accompanied with the visualization of the curvature and inclination profiles along the path are shown in Fig. 3 to demonstrate that the horizontal and vertical turning radii may have two very different values. The curvature of the path depends on the particular turn at the specific part of the path. From the visualized profiles, it can be seen that there is only a little space for further optimization of the found 3D path because the pitch angle is saturated for most of the time. Note that the relative gap of the path length to the determined lower bound is 0.855%.

A. Discussion

It is worth noting that the results for the Numerical [8] are adopted from [7], and for some cases, the reported values are lower than the determined lower bound. Despite an in-depth investigation of possible errors in the used implementation, we did not find any error, and it seems the Numerical method might suffer from numerical stability issues. Besides, for few cases, the proposed method and also RDDH [7] provide better results than the Numerical method, which might also be caused by numerical issues or by an early stop as the Numerical method is claimed to converge to the optimal paths. Because of these reasons, the values of the Numerical method are shown in italic in Table II.

Regarding the computational requirements, the RDDH [7] is reported to run in tens of microseconds on a Pentium-class computer running at $2.2\,\mathrm{GHz}$, while the Numerical method is reported to take about 1.2 minutes in [8]. Our proposed method runs in hundreds of microseconds, which is slightly more than RDDH, but it provides better results in most of the cases and also a relatively tight gap to the newly introduced lower bound. Thus, the proposed heuristic method might provide a suitable choice for finding 3D paths with bounded curvature and pitch angle in real-time with the estimation of the quality of the found solution using the proposed tight lower bound.

Moreover, there is another advantage of the proposed solution that is a generation of paths with fewer turns than, e.g., using the Dubins airplane model [5]. An example of such a difference is depicted in Fig. 1. Although the final path length can be similar, a path with fewer turns may produce benefits such as being more easily followed by the controller.

| Name	LB_{Num} [18]	Proposed lower and upper bounds					RDDH [7]	Numerical[†] [8]	Proposed Heuristic		
		LB	UB	%GAP$_b$	T_{LB} [μs]	T_{UB} [μs]			Length	%GAP	T [μs]
Long 1	**437.86**	433.03	490.31	11.682	8.1	7.8	467.70	*449.56*	**446.04**	1.834	197.9
Long 2	**631.73**	621.97	692.39	10.171	7.1	8.0	649.52	*636.12*	**638.45**	1.052	137.0
Long 3	**1059.20**	1043.98	1099.57	5.056	6.9	7.9	1088.10	*1063.41*	**1068.34**	0.855	178.8
Long 4	**1784.85**	1774.27	1833.51	3.231	7.0	8.0	1802.60	*1789.21*	**1788.80**	0.221	151.7
Long 5	**2213.70**	2201.55	2238.40	1.646	7.0	7.4	2245.14	*2216.40*	**2214.54**	0.038	184.3
Short 1	299.34	**580.70**	—	—	7.2	0.7	588.60	*583.47*	**580.79**	0.015	152.6
Short 2	281.96	**667.24**	—	—	7.7	0.2	**667.71**	*658.53*	668.17	0.140	184.9
Short 3	342.52	**976.34**	—	—	8.3	0.2	979.34	*968.25*	**976.79**	0.047	262.5
Short 4	422.26	**1169.52**	—	—	7.1	0.8	**1169.73**	*1161.55*	1169.80	0.023	228.0
Short 5	437.46	**1362.71**	—	—	7.6	0.2	1367.56	*1354.12*	**1362.91**	0.015	193.5

[†]The values are adopted from [7] and are shown in italic as they depend on the number of intervals taken for the multiple shooting algorithm.
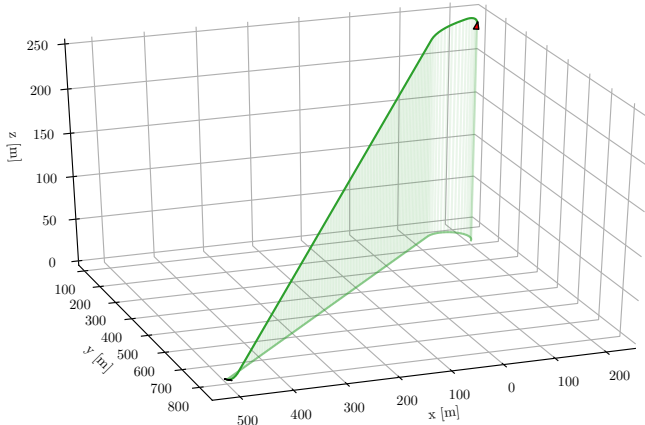
(a) 3D projection of the found trajectory.
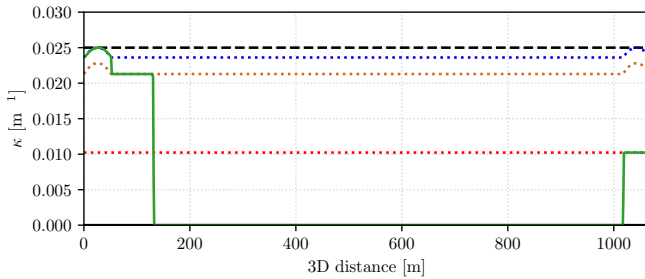
(b) Computed curvature of the found 3D path (green) with its limit (black). Dotted lines represent theoretical curvature computed by (4): brown for the horizontal turn, red for the vertical turn, and blue for the combined turn.
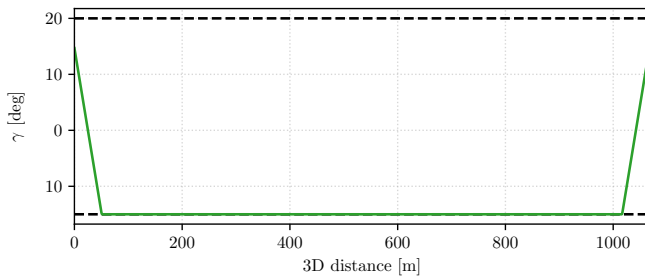
(c) Pitch angle of the found 3D path (green) with its limits (black).

Fig. 3. Example of the computed 3D path by the proposed heuristic approach for the instance Long 3. The minimum turning radius $\rho_{min} = 40$ m and the limit for the pitch angle $\Gamma = [-15°, 20°]$. The results are supplemented with computed curvature and altitude profiles.

The proposed decoupled-based local optimization method represents a relatively simple, yet efficient approach to generalize the existing results on 2D Dubins path into the three-dimensional space while respecting both the maximal curvature and pitch angle constraints of the vehicle. The presented methodology has been numerically evaluated using existing benchmark instances, and the reported results show that the proposed method is competitive to the optimal solution [8]. Besides, it also provides paths with fewer turns than solutions given by other similar state-of-the-art methods like [5], [7], which provides benefits in the path execution.

The work has several directions to be addressed next. One of the directions is to extend the technique to consider environments with obstacles, a scenario that can fit real-world cases. However, a known problem concerning the use of Dubins curves is the discontinuity of the curvature profile, leading to abrupt lateral accelerations. Therefore, we intend to study possible techniques for generating smoother variations of acceleration that can be based on other types of curves such as clothoid [22] or Bézier [23] curves, e.g., that have been already utilized in multi-goal planning in surveillance missions [24].

VI. CONCLUSION

In this paper, we address the problem of finding minimal three-dimensional Dubins path with bounded curvature and pitch angle. The proposed method is based on the decoupled approach to determine two two-dimensional Dubins paths separately for the horizontal and vertical projections of the 3D final path. The initially generated paths are further improved by a local iterative optimization to decrease the length of the final path while still guaranteed the path constraints are met. Moreover, based on the decoupled approach, we propose a computationally efficient method for estimating both lower and upper bounds of the optimal path length that enables to estimate the quality of solutions quickly. Regarding the reported results, the lower bound seems to be relatively tight in comparison to the found feasible solutions. Our future research directions aim to address abrupt lateral accelerations along the Dubins curves, and thus we plan to investigate other curve parametrizations.

REFERENCES

[1] J. Cao, J. Cao, Z. Zeng, and L. Lian, "Optimal path planning of underwater glider in 3d dubins motion with minimal energy consumption," *OCEANS*, pp. 1–7, 2016.

[2] J. Faigl, P. Váňa, R. Pěnička, and M. Saska, "Unsupervised learning-based flexible framework for surveillance planning with aerial vehicles," *Journal of Field Robotics*, vol. 36, no. 1, pp. 270–301, 2019.

[3] D. G. Macharet and M. F. M. Campos, "A survey on routing problems and robotic systems," *Robotica*, vol. 36, no. 12, pp. 1781–1803, 2018.

[4] M. Dunbabin and L. Marques, "Robots for Environmental Monitoring: Significant Advancements and Applications," *IEEE Robotics & Automation Magazine*, vol. 19, no. 1, pp. 24–39, 2012.

[5] M. Owen, R. Beard, and T. McLain, "Implementing Dubins Airplane Paths on Fixed-Wing UAVs," in *Handbook of Unmanned Aerial Vehicles*, K. P. Valavanis and G. J. Vachtsevanos, Eds. Springer Netherlands, 2014, pp. 1677–1701.

[6] L. E. Dubins, "On curves of minimal length with a constraint on average curvature, and with prescribed initial and terminal positions and tangents," *American Journal of Mathematics*, vol. 79, no. 3, pp. 497–516, 1957.

[7] Y. Wang, S. Wang, M. Tan, C. Zhou, and Q. Wei, "Real-Time Dynamic Dubins-Helix Method for 3-D Trajectory Smoothing," *IEEE Transactions on Control Systems Technology*, vol. 23, no. 2, pp. 730–736, 2015.

[8] S. Hota and D. Ghose, "Optimal path planning for an aerial vehicle in 3D space," in *IEEE Conference on Decision and Control (CDC)*, 2010, pp. 4902–4907.

[9] S. M. LaValle, *Planning Algorithms*. New York, NY, USA: Cambridge University Press, 2006.

[10] T. T. Mac, C. Copot, D. T. Tran, and R. De Keyser, "Heuristic approaches in robot path planning: A survey," *Robotics and Autonomous Systems*, vol. 86, pp. 13–28, 2016.

[11] Y. Kuwata, G. Fiore, J. Teo, E. Frazzoli, and J. How, "Motion planning for urban driving using RRT," in *IEEE/RSJ International Conference on Intelligent Robots and Systems (IROS)*, 2008, pp. 1681–1686.

[12] A. Alves Neto, D. G. Macharet, and M. F. M. Campos, "Feasible RRT-based path planning using seventh order Bézier curves," in *IEEE/RSJ International Conference on Intelligent Robots and Systems (IROS)*, 2010, pp. 1445–1450.

[13] S. C. Yun, V. Ganapathy, and L. O. Chong, "Improved genetic algorithms based optimum path planning for mobile robot," in *International Conference on Control Automation Robotics Vision (ICARCV)*, dec. 2010, pp. 1565–1570.

[14] D. G. Macharet, A. Alves Neto, and M. F. M. Campos, "Feasible UAV path planning using genetic algorithms and Bézier curves," in *20th Brazilian Conference on Advances in Artificial Intelligence (SBIA)*, 2010, pp. 223–232.

[15] H. Chitsaz and S. M. LaValle, "Time-optimal paths for a Dubins airplane," in *IEEE Conference on Decision and Control (CDC)*, 2007, pp. 2379–2384.

[16] Y. Lin and S. Saripalli, "Path planning using 3D Dubins Curve for Unmanned Aerial Vehicles," in *International Conference on Unmanned Aircraft Systems (ICUAS)*, 2014, pp. 296–304.

[17] G. Ambrosino, M. Ariola, U. Ciniglio, F. Corraro, E. De Lellis, and A. Pironti, "Path generation and tracking in 3-D for UAVs," *IEEE Transactions on Control Systems Technology*, vol. 17, no. 4, pp. 980–988, 2009.

[18] S. Hota and D. Ghose, "Optimal geometrical path in 3d with curvature constraint," in *IEEE/RSJ International Conference on Intelligent Robots and Systems (IROS)*, 2010, pp. 113–118.

[19] P. Váňa and J. Faigl, "Optimal solution of the generalized dubins interval problem," in *Robotics: Science and Systems (RSS)*, 2018.

[20] A. M. Shkel and V. Lumelsky, "Classification of the dubins set," *Robotics and Autonomous Systems*, vol. 34, no. 4, pp. 179–202, 2001.

[21] P. Váňa, J. Faigl, A. A. Neto, and D. G. Macharet, "Minimal 3d Dubins path with bounded curvature and pitch angle," [cited on 2019-Sep-10]. [Online]. Available: https://github.com/comrob/

[22] M. Shanmugavel, A. Tsourdos, B. White, and R. Żbikowski, "Co-operative path planning of multiple UAVs using Dubins paths with clothoid arcs," *Control Engineering Practice*, vol. 18, no. 9, pp. 1084–1092, 2010.

[23] A. A. Neto, D. G. Macharet, and M. F. M. Campos, "3d path planning with continuous bounded curvature and pitch angle profiles using 7th order curves," in *IEEE/RSJ International Conference on Intelligent Robots and Systems (IROS)*, 2015, pp. 4923–4928.

[24] J. Faigl and P. Váňa, "Surveillance Planning With Bézier Curves," *IEEE Robotics and Automation Letters*, vol. 3, no. 2, pp. 750–757, 2018.